Science of the Total Environment 736 (2020) 137839

Contents lists available at ScienceDirect

Science of the Total Environment

journal homepage: www.elsevier.com/locate/scitotenv

Strong mineralogic control of soil organic matter composition in response to nutrient addition across diverse grassland sites

Qian Zhao [a], Stephen J. Callister [a], Allison M. Thompson [a], Ravi K. Kukkadapu [a], Malak M. Tfaily [a,1], Lisa M. Bramer [b], Nikolla P. Qafoku [c], Sheryl L. Bell [a], Sarah E. Hobbie [d], Eric W. Seabloom [d], Elizabeth T. Borer [d], Kirsten S. Hofmockel [a,e,*]

[a] Earth and Biological Sciences Directorate, Pacific Northwest National Laboratory, 902 Battelle Blvd, Richland, WA 99354, USA
[b] National Security Directorate, Pacific Northwest National Laboratory, 902 Battelle Blvd, Richland, WA 99354, USA
[c] Energy & Environment Directorate, Pacific Northwest National Laboratory, 902 Battelle Blvd, Richland, WA 99354, USA
[d] Department of Ecology, Evolution & Behavior, University of Minnesota, 1479 Gortner Avenue, St. Paul, MN 55108, USA
[e] Department of Ecology, Evolution & Organismal Biology, Iowa State University, 251 Bessey Hall, Ames, IA 50011, USA

HIGHLIGHTS

- Beyond clay content, mineralogy strongly controlled the composition of MAOM.
- Ferrihydrite accumulated proteins and lipids in the hydrophobic zone of MAOM.
- The mineral core influenced biochemical persistence of OM in the kinetic zone.
- Nitrogen fertilization altered carbon chemistry and organo-mineral interactions.

GRAPHICAL ABSTRACT

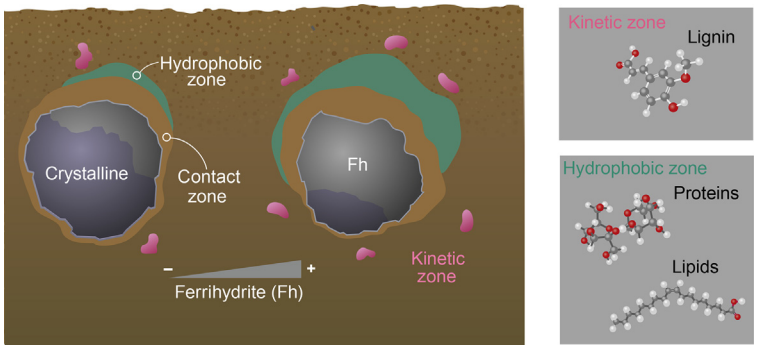

ARTICLE INFO

Article history:
Received 8 January 2020
Received in revised form 4 March 2020
Accepted 8 March 2020
Available online 6 April 2020

Editor: Jay Gan

Keywords:
Organo-mineral complex
Zonal structure
Chemical composition
Mineralogy
Ecosystem service
Fertilization

ABSTRACT

Soil organic matter (SOM) dynamics are central to soil biogeochemistry and fertility. The retention of SOM is governed initially by interactions with minerals, which mediate the sorption of chemically diverse organic matter (OM) molecules via distinct surface areas and chemical functional group availabilities. Unifying principles of mineral-OM interactions remain elusive because of the multi-layered nature of biochemical-mineral interactions that contribute to soil aggregate formation and the heterogeneous nature of soils among ecosystems. This study sought to understand how soil mineralogy as well as nitrogen (N) enrichment regulate OM composition in grassland soils. Using a multi-site grassland experiment, we demonstrate that the composition of mineral-associated OM depended on the clay content and specific mineral composition in soils across the sites. With increasing abundance of ferrihydrite (Fh) across six different grassland locations, OM in the hydrophobic zone became more enriched in lipid- and protein-like compounds, whereas the kinetic zone OM became more enriched in lignin-like molecules. These relationships suggest that the persistence of various classes of OM in soils may depend on soil iron mineralogy and provide experimental evidence to support conceptual models of zonal mineral-OM associations. Experimental N addition disrupted the accumulation of protein-like molecules in the hydrophobic zone and the positive correlation of lignin-like molecules in the kinetic zone with Fh content, compared to unfertilized soils. These data suggest that mineralogy and clay content together influence the chemical

* Corresponding author at: Pacific Northwest National Laboratory, 902 Battelle Blvd, Richland, WA 99354, USA.
E-mail address: kirsten.hofmockel@pnnl.gov (K.S. Hofmockel).
[1]Current at: Department of Soil, Water and Environmental Science, University of Arizona, 1177 E 4th St, Tucson, AZ 85719, USA.

https://doi.org/10.1016/j.scitotenv.2020.137839

composition not only of mineral-associated OM, but also of soluble compounds within the soil matrix. If these relationships are prevalent over larger spatial and temporal scales, they provide a foundation for understanding SOM cycling and persistence under a variety of environmental contexts.

1. Introduction

The retention and accrual of soil organic matter (SOM) are essential for maintaining soil fertility as well as modulating the land-atmosphere exchange of carbon (C). Although decades of studies have addressed the mechanisms regulating soil C sequestration, there remains a need for improved understanding of the factors controlling SOM stabilization at continental to global scales (Rasmussen et al., 2018). Although much research has focused on the physical, chemical and mineralogical characteristics of soils that influence SOM storage (Torn et al., 1997; Schmidt et al., 2011; Kleber et al., 2015), an integrated understanding of SOM persistence remains elusive.

Organic matter (OM) persists in soil when it is inaccessible to microbes because of thermodynamic stability, chemical protection in the form of chemical bonding, or physical protection within the layers of mineral-associated organic matter (MAOM) or larger soil aggregate fractions (Schmidt et al., 2011; Stevenson, 1995; Christensen, 1996; Six et al., 2002). In recent conceptual models, MAOM dynamics are suggested to have the strongest influence on the extent of microbial mineralization vs. long term persistence of soil organic C (Schmidt et al., 2011; Kleber et al., 2007; Luo et al., 2016; Abramoff et al., 2018; Todd-Brown et al., 2013). This is because mineral associations are the most important mechanisms protecting C from microbial respiration for centuries or millennia as they limit microbial and enzymatic access (Kaiser and Guggenberger, 2003; Zimmerman et al., 2004; Conant et al., 2011).

MAOM is a heterogeneous pool comprised of diverse organic molecules and varied mineral constituents. Characterization of this diversity has largely been done operationally. As one example, MAOM is commonly isolated in fine particles (<53 μm), such as silt and clay, because the equivalent spherical diameter of minerals in mineral-OM complexes is typically <2 μm ("clay-size fraction") (Kleber et al., 2015). Previous studies suggest that the clay-size fraction protects SOM from decomposition because of its high mineral content and large specific surface area, compared with silt and sand-size fractions (Six et al., 2002; Krull et al., 2001; Xu et al., 2016). Therefore, soil clay content (the mass of the clay-size fraction) is extensively used to predict the preservation of SOM via mineral-OM interactions. However, the clay-size fraction of soil consists of diverse mineral phases, including phyllosilicates and metal oxides (Kaiser et al., 1997; Sposito et al., 1999; Lopes and Guilherme, 2016), which provide the chemical foundation for varied interactions between specific minerals and OM functional groups (Rasmussen et al., 2018). Recent findings demonstrated that other physicochemical parameters, such as, exchangeable Ca and Fe- and Al-oxyhydroxides, emerged as better predictors of SOM content, with clay content having relatively little explanatory power (Rasmussen et al., 2018; Torn et al., 1997; Coward et al., 2017; Yu et al., 2017).

Among the diverse mineral phases, iron (Fe) bearing minerals are considered to dominate in OM preservation, contributing between 3 and 72% of total organic C in soil and sediment depending on mean annual precipitation and potential evapotranspiration (Wagai and Mayer, 2007; Lalonde et al., 2012; Zhao et al., 2016; Kramer and Chadwick, 2018). Ferrihydrite (Fh, a type of short-range ordered Fe oxides) is likely an important Fe mineral for C stabilization because of its reactive nature and higher sorption affinity to OM compared to highly crystalline minerals (e.g., goethite and hematite) (Bigham et al., 2002; Lv et al., 2016). A number of previous studies have applied physical and chemical approaches to distinguish the MAOM pools and their chemical features (Coward et al., 2017; Rumpel et al., 2012; Hatton et al., 2012; Jones and Singh, 2014; Heckman et al., 2018; Huang et al., 2018). For example, agricultural soil extracted by oxalate revealed that short-range ordered Fe oxides preferentially retain aromatic organic compounds (e.g., lignin molecules) (Huang et al., 2018). Further, experiments assessing the sorption of dissolved OM onto pure mineral surfaces revealed that short-range ordered Fe minerals selectively adsorbed aromatic compounds (e.g., lignin molecules), whereas high-crystalline minerals associated with aliphatic OM (e.g., hydrocarbons, carbohydrates) (Coward et al., 2018). These different approaches highlight the challenge to develop an integrated understanding of how mineral composition regulates MAOM in soil.

Further challenges in understanding mineral-OM interactions arise from the zonal nature of those interactions. Recent conceptualizations of MAOM recognize three such zones (Six et al., 2002; Kleber et al., 2007): the "contact zone" of MAOM is persistent and unavailable to microbial enzymes; the "hydrophobic zone" comprises nonpolar molecules with low solubility in water that are chemically sorbed to the contact zone OM or directly to mineral surfaces; and the "kinetic zone" refers to OM that is loosely bound to organo-mineral complexes (Fig. 1). OM in both the hydrophobic and kinetic zones is considered "dynamic pool" which can either be accessible to microbial enzymes or can persist and contribute to the "static pool" (as in the "contact zone") (Kleber et al., 2007). OM in the outer layer (kinetic zone) is decomposed by microbial enzymes (and thus its persistence is mainly driven by biochemical stabilization), whereas OM in the inner layer (contact zone) is stabilized by sorption to mineral surfaces. It has been suggested that the mineral core of soil aggregates has a finite capacity to sequester C in the contact zone via organo-mineral complexes (e.g. C saturation hypothesis) (Six et al., 2002). Additional protection of SOM can occur through the sorption in the hydrophobic zone, or occlusion within microaggregates, and even through biochemical persistence in the kinetic zone (Six et al., 2002; Kleber et al., 2007).

Yet, in order to extract MAOM, many studies use organic solvents, e.g. dithionite or ammonium oxalate, that disturb mineral structures by reductive dissolutions or acid digestions. These extractions are unable to isolate the composition of different MAOM layers, including the outer layers of MAOM, where biological C decomposition occurs. As a result, the extent to which the mineral core of soil aggregates influences the chemistry (and ultimately the persistence) of OM in different C pools of whole soil remains poorly understood. Yet such understanding is critical because mineral-OM interactions impact substrate availability for plants and microbes, including access to limiting nutrients, as well as potential loss of C and nutrients to the atmosphere or surface and groundwater systems.

In addition to soil mineralogy, MAOM responses to nitrogen (N) fertilization are important to understand, as land use shifts grasslands to agroecosystems, where fertilization may influence the cycling and long-term storage of MAOM. For instance, inorganic nutrient sorption to mineral surfaces can compete with OM sorption by blocking sorption sites (Churchman and Lowe, 2012; Havlin et al., 2005; Sparks, 2003; Mikutta and Kaiser, 2011; Schneider et al., 2010); and N-induced acidification strongly affects mineral-OM interactions by influencing mineral surface reactivity and soil cation chemistry (Ye et al., 2018). N fertilization alters soil microbial communities that may affect the cycling of OM and minerals and thus the turnover of MAOM (Leff et al., 2015). Thus, evaluating the response of mineral-OM interactions to nutrient enrichment will help to increase the understanding of mechanisms that drive coupled C and nutrient biogeochemical cycles at the interface with minerals.

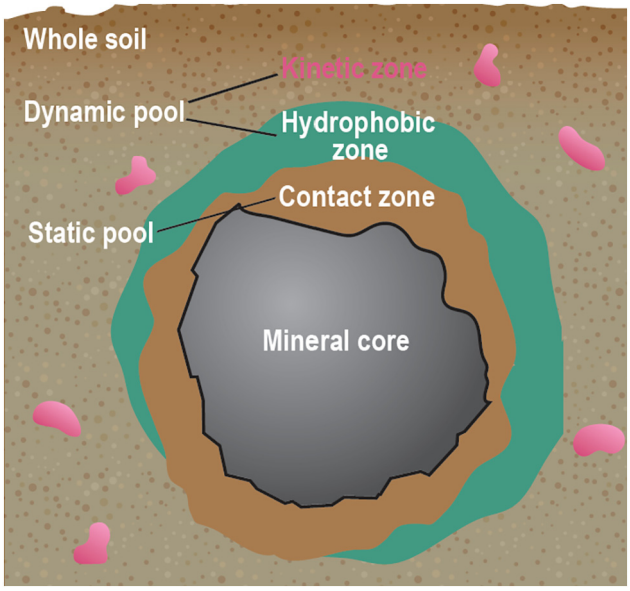

Fig. 1. Zonal structure of organo-mineral complexes. Organo-mineral complexes consist of "dynamic" and "static" pools, where the "dynamic" pool includes "kinetic" and "hydrophobic" zones and the "static" pool refers to the "contact" zone. "Dynamic" and "static" pools are distinguished by both mean residence time and accessibility to microbial enzymes.

This study addresses the role of soil mineralogy and N enrichment in influencing the composition of MAOM and nature of mineral-OM interactions across six North American grassland sites. Specifically, we hypothesized that Fh would stabilize OM enriched in hydrophilic functional groups because of the high surface area and prevalent hydroxyl (OH) groups of Fh (Kaiser and Guggenberger, 2000). We hypothesized that the addition of N-fertilizer would enrich N-containing functional groups on OM surfaces and alter the surface charges of OM likely via N-induced acidification. By combining an ecosystem-scale experiment with ultra-high resolution biogeochemical data, we were able to characterize the mineral-OM interactions at the molecular scale, and for the first time, provide empirical evidence for the zonal structure of MAOM in natural grassland ecosystems. Further, our results demonstrate that chronic N fertilization disrupts predicted relationships, resulting in a new conceptual model of how MAOM stabilization is influenced by mineralogy and N enrichment.

2. Material and methods

2.1. Study sites and soil sampling

Study sites were located in the Central Great Plains and Oregon, USA, and are a part of the Nutrient Network (NutNet) (Borer et al., 2014) study, a global ecosystem-scale nutrient addition field experiment replicated at over 100 grassland sites in 25 countries on five continents (Borer et al., 2014). Our six focal sites were chosen to span a wide range of total C (0.3–18.6 wt%), total Fe (1.0–7.5 wt%), and clay content (0.8–9.8%) (Fig. 2, Table 1 for unfertilized and Table S1 for N-fertilized soil). Five soil orders, including Andisols (LK), Inceptisols (BG), Aridisols (SV), Entisols (SG & CC), and Mollisols (CP), were included in these six sites, providing dissimilar pedogenic processes. At each site, we collected soil from two separated plots, unfertilized control plot and N-fertilized plot (10 g N m^{-2} yr^{-1} timed-release urea) for at least eight years prior to sampling in 2016. Treatments were assigned in a completely randomized block design (3–6 blocks per site) (Borer et al., 2014). The top 15 cm of soil was collected and a total of 15 g of soil composited from three 1 cm inner-diameter soil cores at three random locations in each plot. Soil was sealed in plastic bags and shipped with dry ice to the lab where field-moist soil was composited within a plot, sieved through 2 mm mesh, and roots were removed. Soil was stored in 50 ml Falcon tubes at −80 °C until further analyses. Soil characterization data, including pH, soil texture, and moisture, were provided by Nutrient Network collaborators at https://nutnet.org/data. Soil pH was determined in 1:1 soil:water suspension. Soil texture was determined by the pipette method (Gee and Bauder, 1986). The clay content was calculated by % of clay to the whole soil on mass basis. Total C and N % were measured by a Vario EL Cube CHNS elemental analyzer from Elementar Americas, Inc. (Ronkonkoma, NY, USA) on dry mass basis. Total contents of other elements (Al, Fe, Mg, P, Si) were measured by acid digestion in Nitric acid and Hydrofluoric acid, followed by ICP-OES. Microbial biomass C content was measured by a modified sequential chloroform ($CHCl_3$) fumigation direct extraction method (Witt et al., 2000; Hofmockel et al., 2007). Briefly, 8 g of soil was mixed with 24 ml of a 0.5 M K_2SO_4 solution in a 50 ml falcon tube. Samples were shaken at 200 rpm at 20 °C for 2 h. Then, soil slurry was centrifuged and filtered through pre-leached ashless filter paper (Whatman grade 42). $CHCl_3$ was added directly to the soil pellet and filter from the initial extraction and samples were fumigated for 48 h. Fumigated samples were re-extracted with K_2SO_4 under the same conditions. Non-purgeable C in the acidified extracts were quantified using a vario TOC Cube (Elementar, Germany).

2.2. Mineralogy

Variable temperature ^{57}Fe- Mössbauer spectroscopy were used to determine Fe mineral composition (Section S1). Powder X-ray powder diffraction (XRD) and elemental analysis on Al, Si, Fe, and P were measured to provide supportive information for Mössbauer spectroscopy to determine mineral composition. Variable temperature ^{57}Fe-Mössbauer spectroscopy measurements of ~100–150 mg of the each sample mixed with powdered sugar were performed using a WissEl Elektronik (Germany) or a Web Research (Edina, MN) instrument that included a closed-cycle cryostat SHI-850 obtained from Janis Research Co., Inc. (Wilmington, MA), a Sumitomo CKW-21 He compressor unit, and an Ar-Kr proportional counter detector (LND, Inc. NY). Details in parameters of the measurement can be found in Section S1 from Supplementary Information. The Mössbauer spectroscopy data were modeled using a Voigt-based hyperfine distribution model, Rancourt and Ping (1991) (Recoil software, University of Ottawa, Canada). The sample preparation was identical to the procedures reported in Peretyazhko et al. (2012). The rationale behind obtaining Mössbauer spectra at various temperatures to characterize the suite of Fe minerals in a sample is discussed in Section S1. The proportions and concentrations of Fe mineral phases from unfertilized plots from the six sites are summarized in Table S2. We assumed the same proportions and concentrations of each Fe mineral phase in soils from N-fertilized and unfertilized plots because minimal differences between them were found from 5 K Mössbauer spectra of two soils (Fig. S1).

2.3. Hydrophobic and kinetic zone OM analyses

The dynamic pool (hydrophobic + kinetic zone) of SOM is the focus of this study as it is subject to biogeochemical processes, whereas the static pool (contact zone) is stable and unavailable to microbial transformations (Fig. 1). Here, we used sequential water (H_2O) and a mixture of methanol (MeOH) and $CHCl_3$ to selectively extract specific compound classes (Tfaily et al., 2015; Tfaily et al., 2017). Extracts were analyzed by Fourier transform ion cyclotron resonance mass spectrometry (FTICR-MS) to characterize the chemical composition of the dynamic pool of SOM (see Section S2 for details regarding sample preparation and data acquisition). Water extraction (30% w/v) releases the fractions of labile and polar OM that are unbound and/or loosely bound to MAOM. Water extraction organic matter (WEOM) comprises

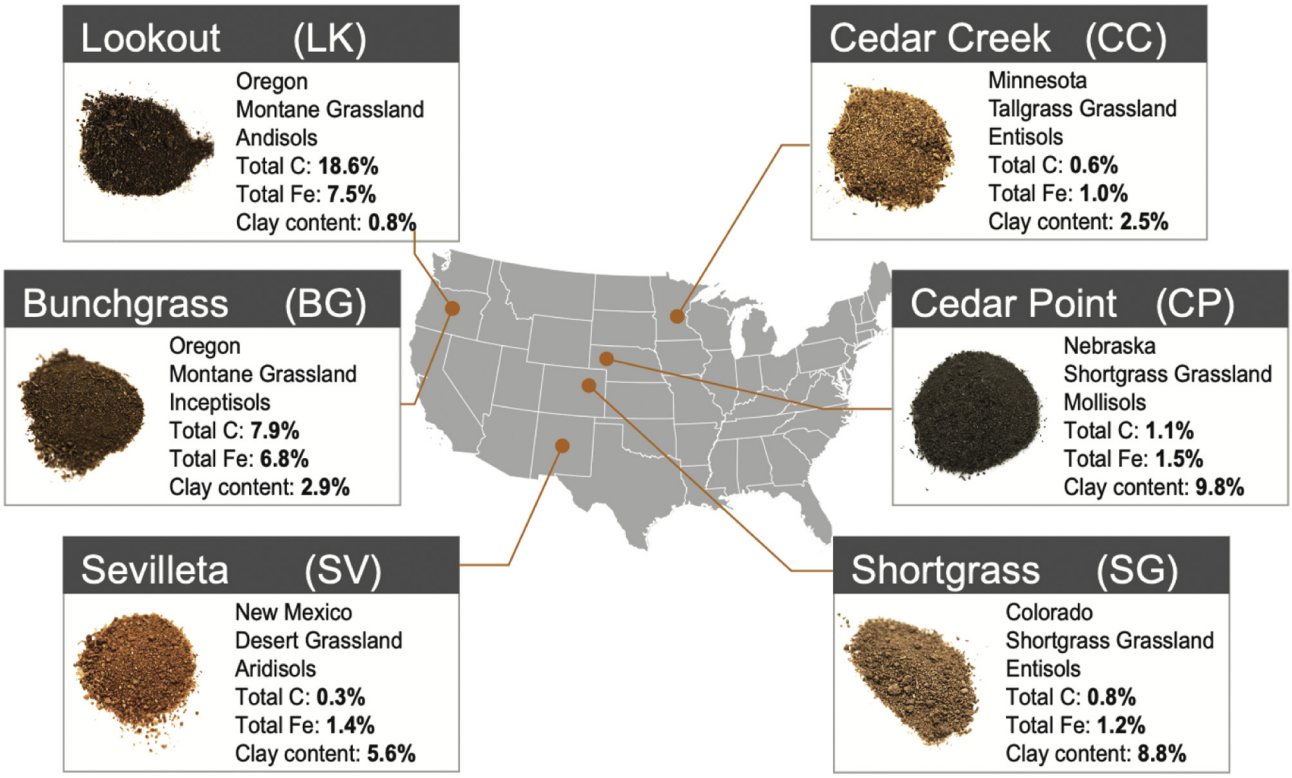

Fig. 2. Locations of six study sites from the Nutrient Network project with site information and soil properties.

compounds easily accessed by plants and microbes, and therefore reflect the "kinetic zone" from the zonal structure of organo-mineral complexes (Kleber et al., 2007). Next, a mixture of MeOH and $CHCl_3$ extraction was performed and finished with two separated layers of extracts, where MeOH extracts polar to semi-polar compounds similar to H_2O (Tfaily et al., 2015; Tfaily et al., 2017); as a result, we did not present MeOH extracts. $CHCl_3$ extraction is selective for hydrophobic organic compounds (ranging from semi-polar to non-polar compounds) (Folch et al., 1957), and therefore approximates the "hydrophobic zone" from the zonal structure of organo-mineral complexes (Kleber et al., 2007). Although $CHCl_3$ extraction may likely include hydrophobic compounds from organic residues (non-MAOM), this fraction is presumably minimum or proportional to the "hydrophobic zone" of MAOM (von Lützow et al., 2008). Both H_2O and $CHCl_3$ extractions are operationally defined to target OM that can be extracted from soils without disrupting minerals, and therefore represents organic

Table 1
Characteristics of 6 unfertilized study sites, located in the Central and Intermountain Western USA.

Site name	Lookout ridge, OR ($n = 3$)	Bunchgrass, OR (n = 3)	Sevilleta LTER, NM (n = 4)	Cedar creek LTER, MN (n = 5)	Shortgrass steppe LTER, CO (n = 3)	Cedar point biological station, NE ($n = 6$)
Abb.	LK	BG	SV	CC	SG	CP
Habitat	Montane grassland	Montane grassland	Desert grassland	Tall grass prairie	Short grass prairie	Short grass prairie
Soil order	Andisols	Inceptisoles	Aridisols	Entisols	Entisols	Mollisols
Latitude (°)	44.2	44.3	34.4	45.4	40.8	41.2
Longitude (°)	−122.1	−122.0	−106.7	−93.2	−104.8	−101.6
Elev. (m)	1500	1318	1600	270	1650	965
MAP (mm)	898	647	52	50	65	45
MAT (°C)	4.8	5.5	12.6	6.3	8.4	9.5
Moisture (%)	37.6	24.6	4.1	6.6	9.2	3.2
pH	4.9	5.7	8.4	6.1	6.6	7.2
Clay (%)	0.8	2.9	5.6	2.5	8.8	9.8
Silt (%)	30.1	26.5	9.9	8.1	17.1	19.9
Sand (%)	69.0	70.4	84.4	89.3	74.0	70.2
Total C (%)	18.6	7.9	0.3	0.6	0.8	1.1
Total N (%)	1.26	0.54	0.03	0.04	0.08	0.1
C/N	14.8	14.7	11.0	13.3	9.77	11.4
Total Al (%)	11.37	11.25	4.9	4.07	4.55	5.36
Total Fe (%)	7.5	6.83	1.44	0.95	1.15	1.46
Total Mg (%)	1.27	2.6	0.35	0.18	0.25	0.37
Total P (%)	0.5	0.22	0.02	0.03	0.03	0.03
Total Si (%)	15.22	16.07	32.8	36.21	35.16	34.59
C/Fe (mol/mol)	11.9	6.0	0.88	5.5	3.7	3.8

MAP, mean annual precipitation; MAT, mean annual temperature; soil pH, moisture, and texture from Nutrient Network collaborators.

molecules that can be accessed by soil microbes. Given that aggregates are dynamic in nature (Six et al., 2000), we chose to focus on extractable pools that directly relate to conceptual models (Kleber et al., 2007), rather than fractionating by size or density (Bach and Hofmockel, 2014). We acknowledge that there are other extraction methods (dithionite, HCl-hydroxylamine, ammonium oxalate, and sodium pyrophosphate) targeting a larger pool of MAOM; however, they intend to disrupt mineral phases by reductive dissolutions or acid digestions (Coward et al., 2017; Heckman et al., 2018), and thus extract the static as well as the dynamic pool of OM.

2.4. FTICR-MS data acquisition

Ultrahigh resolution characterization of OM in the H_2O and $CHCl_3$ fractions was done using a 12 Tesla Bruker SolariX FTICR-MS (see Section S2 for details regarding sample injection parameters). van Krevelen diagrams were constructed to aid in the interpretation of chemical formulas assigned to FTICR MS datasets. They provide a means to visualize and compare the average properties of OM and assign compounds to the major biochemical classes (i.e., lipid-, protein-, lignin-, carbohydrate-, and condensed aromatic-like). Boundaries of classes on the van Krevelen diagram were taken from the boundaries given in Kim et al. (2003), based on the ratios of H to C and O to C. The class defined as 'other' contains any peak which fell outside of the defined boundaries.

2.5. Statistical analysis

Relative contributions of the chemical classes were calculated by taking the count of assigned peaks of each class, divided by the count of total assigned peaks in a specific sample. Statistical analyses were conducted using R software (https://www.r-project.org/). To examine differences in OM composition among sites and treatments, we constructed a Jaccard dissimilarity matrix for all *m/z*'s identified (i.e., both assigned and unassigned peaks) for each solvent ('metaMDS' function from the *vegan* package in R) and class vectors were fit using 'envfit' from *vegan* (Oksanen et al., 2013). Differences between sites were tested with PERMANOVA using 'adonis' (999 permutations, 'vegan') and visualized using Non-metric Multidimensional Scaling (NMDS, 'vegan'). To test significant relationships between relative contributions of certain SOM classes and clay content/Fh content, we fit a generalized linear model with a gamma distribution.

3. Results & discussion

3.1. OM persistence regulated by clay content and beyond

Soil texture (specifically clay content) is a parameter that is often used to predict the C storage capacity of soil ecosystems, and previous results from a variety of ecosystems demonstrate positive correlations between clay content and soil C content (Six et al., 2002; Krull et al., 2001; Xu et al., 2016). By contrast, across the range of soil orders within the NutNet sites studied here, clay content and total C were negatively correlated ($p = 0.014$, $R^2 = 0.78$) (Fig. 3). This negative correlation was driven by the two Oregon sites (LK, BG), which contained high C concentrations (186.3 ± 11.1 mg/g soil for LK, 78.6 ± 9.7 mg/g soil for BG) despite low clay contents (0.8% for LK and 2.9% for BG) compared to those of the Midwestern grasslands (Fig. 2). Without LK and BG, the other four sites showed a significant positive correlation of total C content with the clay content (Fig. S2, $p = 0.003$, $R^2 = 0.44$), consistent with other studies. Our results reinforce that clay content is important in influencing soil C but cannot always accurately predict the C storage capacity of soils across a broad range of sites. Previous study reported that the clay-size fraction consists of a number of minerals, e.g. goethite, hematite, ferrihydrite, kaolinite, and gibbsite (Lopes and Guilherme, 2016), with variable charge surfaces. The positively and negatively charged mineral surfaces can sorb negatively charged OM directly and via polyvalent cation bridging, respectively (Mikutta et al., 2007). In addition, the clay-size fraction has a higher specific surface area for interacting with OM than silt and sand-size fractions (Saggar et al., 1996). LK and BG are distinct from the other four sites in having soils classified as Andisols (formed in volcanic ash containing an abundance of amorphous colloidal materials (Parfitt and Clayden, 1991)) and Inceptisols, respectively. Both of these young grassland soils are enriched in amorphous colloidal materials with high surface areas, which could have contributed to high total C contents.

Similarly, across all sites, microbial biomass C was negatively correlated with clay content (Fig. 3, $p < 0.001$, $R^2 = 0.65$). However, in contrast to total C content, microbial biomass C of the four Midwestern sites was negatively correlated with clay content even after removing LK and BG (Fig. S2, $p < 0.001$, $R^2 = 0.38$). This finding suggests that microbial and total soil C may interact with clay content in different ways. Previous studies demonstrated that phyllosilicates, dominated in clay-size fraction, inhibit the growth of microbes in soil (McMahon et al., 2016; Wong et al., 2004; Wu et al., 2014; Liu et al., 2016a). The underlying mechanisms may be related to the toxicity of metal cations, particularly Al^{3+} and Fe^{2+} (Wong et al., 2004; Morrison et al., 2016). Inhibited microbial growth results in the reduction of microbial C content, supporting to the negative correlation from Fig. 3.

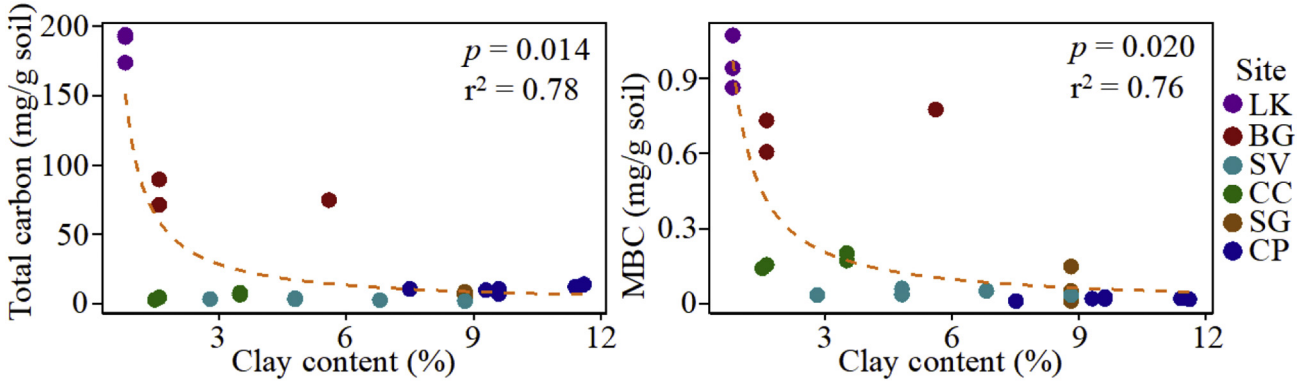

Fig. 3. Correlations between clay content and total soil C content (left) and microbial biomass C (MBC) content (right) from six unfertilized soils. Note: the extractable MBC content (0.26 mg/g soil) only contributes 0.5% of total soil C content (52.5 mg/g soil).

Although the relationship between total C and clay content is depended on which soil orders were included in the analysis, the relationship of specific chemical classes of OM with clay content was consistent for OM in both the kinetic and hydrophobic zones across the six grassland soils. In the hydrophobic zone, the richness of carbohydrate, condensed hydrocarbon, and tannin-like molecules increased with increasing clay content (Fig. S3, $p < 0.05$), whereas lipid and protein-like molecules decreased (Fig. S3, $p < 0.01$). In the kinetic zone, the richness of amino sugar and carbohydrate-like molecules increased with increasing clay content (Fig. S3, $p < 0.05$), and lignin and tannin-like molecules decreased (Fig. S3, $p < 0.05$). In the kinetic and hydrophobic zones, opposite correlations with OM and clay content were observed for tannin compounds (Fig. S3). With increasing clay content, tannins declined in the kinetic zone but increased in the hydrophobic zone. However, carbohydrates consistently increased with increasing clay content in both hydrophobic and kinetic zones. Therefore, the clay content in soil regulates the OM chemical composition in the dynamic pool of MAOM. However, the clay-size fraction is a mixture of minerals with variable charges on their surfaces in general. More detailed information on mineral compositions, specifically Fe minerals/oxides, is essential to understand mechanisms on how Fe minerals interact with each class of organic molecules.

3.2. Mineralogy is the core of organo-mineral complexes

Because the clay-size fraction is a mixture of minerals, additional information on the specific mineral phases, e.g. Fh, is required to interpret the contrasting relationships with clay among different subsets of soil orders and to enhance our understanding of how specific mineral phases control the chemical composition of MAOM. Fe minerals have been reported to protect a significant amount of C in soil and sediment (Wagai and Mayer, 2007; Lalonde et al., 2012; Zhao et al., 2016). Thus, variable-temperature ^{57}Fe Mössbauer spectroscopy was used to determine specific Fe mineral composition (Fig. 4; Figs. S4–S6; Tables S2–S8; see S1 for the determination of Fe mineralogy). In our study, the younger volcanic-derived Andisol and Inceptisol soils (LK and BG) had higher contents of each Fe mineral phase compared to the more developed Aridisols, Entisols and Mollisols (Fig. 4 and Table S2). In particular, Fh was predominant in these two young soils (LK and BG), which is widely known from previous studies. Fh is commonly found in young soils (<10,000 years old) and can be transformed over time to more crystalline structures of Fe oxides, such as goethite or hematite (Cornell and Schwertmann, 2003; Thompson et al., 2006; Chen et al., 2015). Fh has been extensively investigated for its high affinity to sorb OM (Bigham et al., 2002; Chen et al., 2015; Kukkadapu et al., 2004; Adhikari et al., 2017). Although the contents of Fh in SV and CC were much lower than that in LK and BG, the proportional abundance in SV (27%) and CC (33%) were comparable to those from LK and BG (Fig. 4). In addition, SV had the highest proportion of hematite or magnetite (39%) among all sites (Fig. 4). Hematite has been shown to interact with phospholipids via organic phosphate groups and to promote aggregation in the presence of OM (Cagnasso et al., 2010; Liu et al., 2016b). The other two soils (from CP and SG) were dominated by silicate-associated Fe minerals (~55% of total Fe) but had no Fh content (Fig. 4). Silicate-associated Fe minerals interact less with SOM because of the lack of surface active sites compared to Fe oxides. Overall, we found a wide range of contents of each Fe mineral phase from six grassland soils, indicating diverse mineralogy across ecosystems.

In soils from this suite of NetNet sites, clay content (the mass of clay-size fraction of soil) was positively correlated with the proportion of Silicate-Fe ($p < 0.001$, $R^2 = 0.83$) and negatively correlated with the proportion of Fh ($p < 0.001$, $R^2 = 0.83$) (Fig. 5). These correlations suggest that soil with high clay content contains a high proportion of highly crystalline Fe-bearing minerals (e.g. silicate-Fe) but a low proportion of poorly crystalline Fe oxides (e.g. Fh). Weathering is most likely responsible for the mineral transformation, where more fine particles are generated (Dontsova, 2009), and amorphous phases are transformed to highly crystalline phases (Cornell and Schwertmann, 2003; Thompson et al., 2006; Chen et al., 2015). For instance, two young Andisol and Inceptisol soils (LK and BG) had low clay contents and high Fh

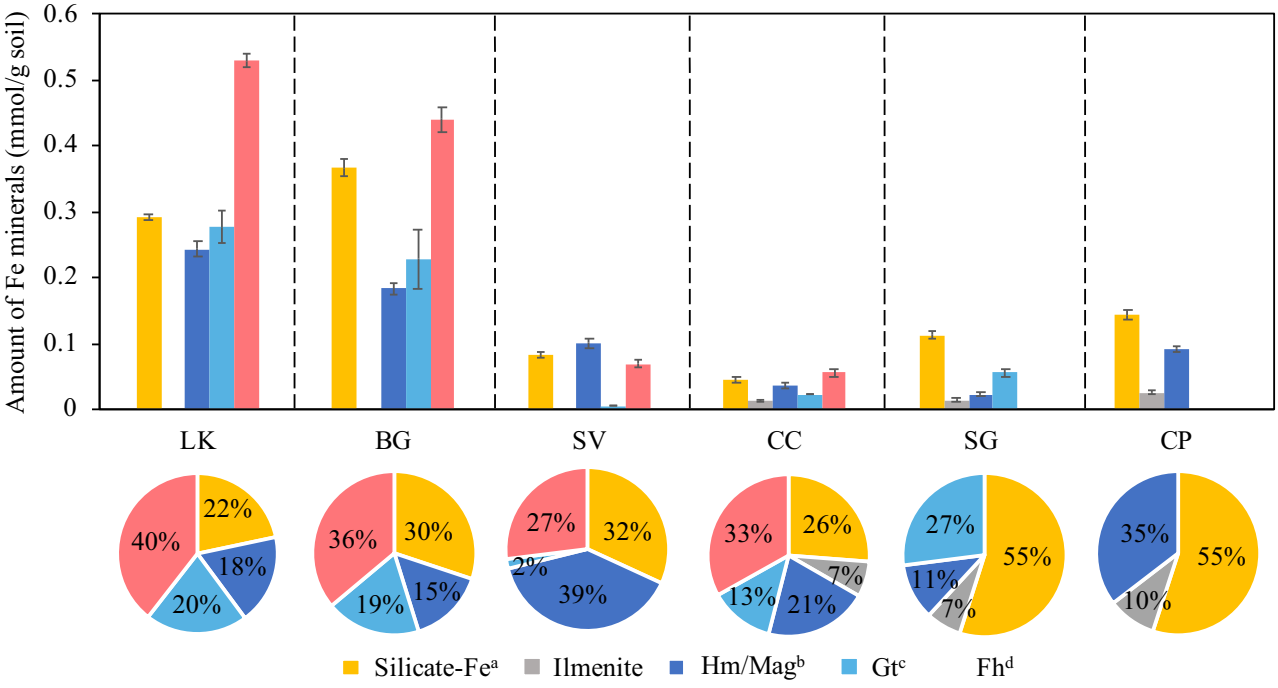

Fig. 4. The amount of Fe mineral phases derived from Mössbauer spectroscopy for six unfertilized soils, arranged by decreasing amount of ferrihydrite. Pie chart shows the proportions of Fe mineral phases. [a]Fe(II) and Fe(III) in silicate minerals (silicate-Fe), [b]"large"-particle hematite/magnetite and Al-hematite (Hm/Mag), [c]nano-/micro-particle or Al substituted goethite (Gt), and [d]ferrihydrite (Fh). Fe mineral concentrations (mmol/g soil) = total Fe content (wt. %) of each soil (chemically determined, Table S1) × proportions of each Fe mineral phase (Mössbauer data, Table S2) / molecular weight of Fe (56 mg/mmol). Error bars represent 2σ standard deviation of proportions of each Fe mineral phase from modeled Mössbauer spectra in Table S3–S8.

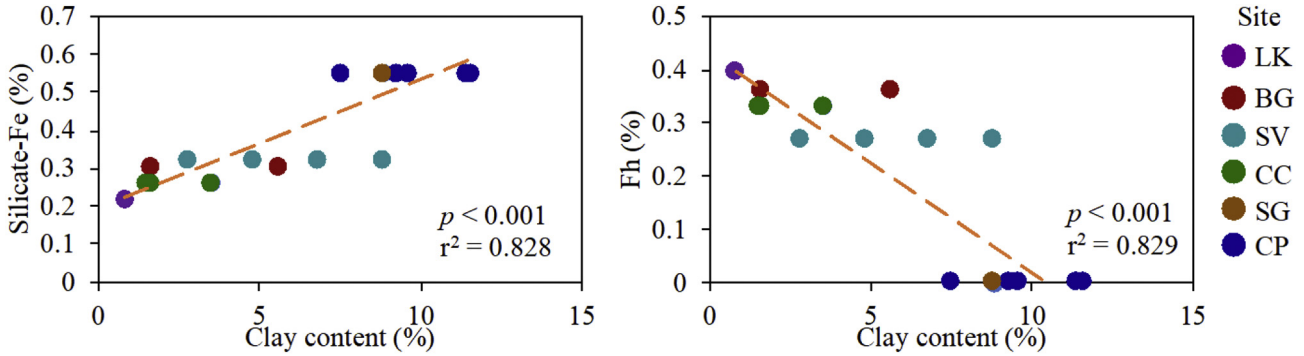

Fig. 5. Correlations between clay content and silicate-Fe (%) (left) and Fh fraction (%) (right) across soils from six unfertilized sites.

proportions, whereas well-developed soils from CP and SG sites were dominated by silicate-Fe minerals. Therefore, the accumulation of OM across grasslands may depend on the type and amount of Fe minerals beyond the clay content. The abundance and composition of different Fe minerals strongly influence the chemistry and content of OM and importantly provide insight into the chemical interactions that are causing OM to persist in grassland soils (Rasmussen et al., 2018). For instance, Fh may exhibit distinct correlations with OM chemical classes, compared with the clay-size fraction due to its high surface area and prevalent OH groups on the surface (Fig. S3) (Kaiser and Guggenberger, 2000).

3.3. Ferrihydrite stabilizes hydrophobic protein and lipid class compounds

Across the six grassland sites, Fh abundance was positively correlated with the relative contribution (% of the number of compounds assigned to each chemical class to the total number of assigned compounds in a sample) of protein-like ($p = 0.03$, $n = 24$) and lipid-like ($p = 0.009$, $n = 24$) compounds in the hydrophobic zone (Fig. 6; Fig. S7; Table S9), reflecting the contrasting mineralogy of the two Fh-rich grasslands in Oregon (0.44–0.52 mmol Fh/g soil) compared to the low Fh content of the Midwestern grasslands. There are a variety of mineral-OM interactions of varying bonding strength that can sorb proteins to the inner OM layer (contact zone) or directly to Fe minerals, including hydrogen bonding, ionic bonding, cation exchange, and polarity. Since proteins are amphiphilic molecules containing both polar and nonpolar functional groups at the amino acid side chains (Hlady and Buijs, 1996), protein molecules can sorb to both hydrophobic and hydrophilic OM functional groups or Fe minerals surfaces via polarity (Fernandes de Oliveira et al., 2005; Quiquampoix et al., 1993). For example, both positively and negatively charged side chains of proteins can sorb to the charged OM layer or mineral surfaces through electrostatic interactions (Johnston et al., 2011). Although the contact zone was proposed as the inner layer and the hydrophobic zones as the outer layer of MAOM (Fig. 1), it is possible that some molecules in the hydrophobic zone of MAOM directly interact with the mineral surface by electrostatic interactions. To consider both cases, we stated that proteins in the hydrophobic zone may sorb to the contact zone or directly to Fe mineral surfaces. Accordingly, OM from the hydrophobic zone contained more N-containing compounds (most likely referring to proteins) compared to OM in the kinetic zone, and the numbers of N-containing compounds in OM from the hydrophobic zone increased with Fh content across the six unfertilized soil types (Fig. S8). In addition, the average C/N ratios for kinetic zone OM are 32.3–59.3 across six sites, while that for hydrophobic zone are 7.6–13.8. These ratios were calculated by the average of C to N atom ratios from the stoichiometry of all assigned formula based on FTICR-MS data of a single grassland site. Although these ratios were not determined by direct measurements, they provide relative comparations of C/N ratios between two zones of MAOM. Our results suggest the preferential accumulation of proteins in the hydrophobic zone of the mineral-OM complex in soils with higher Fh content. Such preferential accumulation of proteins is supported by both conceptual models (Kleber et al., 2007) and computational simulations (Andersen et al., 2016) demonstrating low C:N ratios in hydrophobic zone OM, compared to OM in the kinetic zone.

Based upon the conceptual model of zonal structure of organo-mineral complexes, a hydrophobic zone enriched in phospholipid molecules is formed by connecting hydrophilic regions at the end of hydrocarbon chains with the contact zone (Kleber et al., 2007). By demonstrating that protein and lipid-like compounds preferentially accumulate to the hydrophobic zone of Fh-OM complexes likely due to electrostatic interactions, and suggesting low biogeochemical reactivity and bioavailability of such OM constituents (Stenson et al., 2003; Koch and Dittmar, 2006; Koch and Dittmar, 2016), this study, for the first time, provides empirical evidence from grassland soils to support the zonal structure of MAOM proposed by Kleber et al. (2007) (Fig. 7). Identification of the specific chemical classes that make up the kinetic and hydrophobic zones of MAOM from various soil orders revealed the consistent influence of mineralogy on the nature of SOM.

At first glance, our results seem counter to previous studies (using dithionite extraction) showing that aromatic C was positively and lipids and proteins negatively correlated with Fh (Coward et al., 2017; Zhao et al., 2016; Kramer et al., 2012). This discrepancy highlights that much of our understanding of MAOM is based on chemical pools that are operationally defined, making it difficult to compare across studies. By using a sequential extraction method, we were able to differentiate pools of SOM that were lumped in one-pool approaches (Fig. 1) and thus focus on the dynamic pool of OM (in the kinetic and hydrophobic zones) that is subject to biogeochemical transformations. Our results suggest that even the suite of compounds accumulating beyond the contact zone is influenced by Fh content. This influence likely arises because molecules selectively adsorbed to mineral surfaces in the contact zone influence not only adjacent layers of OM sorption in the hydrophobic zone, but also what is not sorbed and therefore readily dissolved and transported in the kinetic zone. Continuing to elucidate the multi-zonal structure of MAOM will improve understanding of how minerals accrue and stabilize SOM.

The abundance of Fh in unfertilized soils not only led to the accumulation of protein- and lipid-like molecules, but also was negatively associated with amino sugar-, carbohydrate-, condensed hydrocarbon-, lignin-, and tannin-like compounds ($p < 0.05$, $n = 24$, Fig. 6 and Table S9) in the hydrophobic zone of mineral-OM complexes, providing further evidence that the presence of Fh strongly influences the composition of OM that accumulates in grasslands. Condensed hydrocarbons known as polycyclic aromatic hydrocarbons (PAH), lignin from plant cell walls, and tannins that consist of polyphenolic biomolecules from plant litter are normally considered hydrophobic because of the abundance of aromatic rings in their chemical structures. Thus, these hydrophobic molecules tend to cluster together in hydrophilic solvents (water), forming rapid diffusion-limited cluster-cluster aggregates

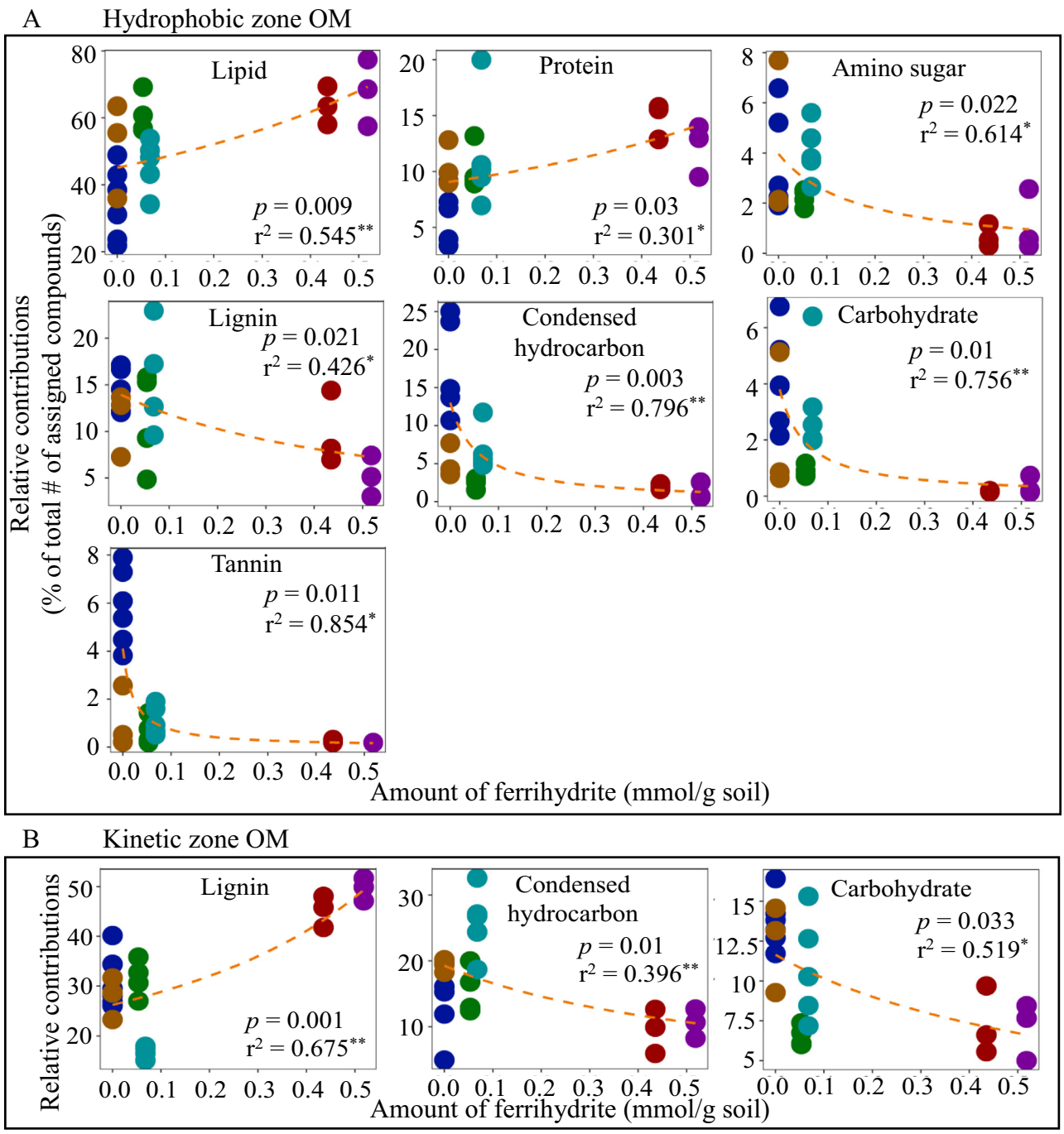

Fig. 6. Correlations of C chemical classes with the amount of ferrihydrite observed for six unfertilized soils collected from grassland sites located throughout the United States. Statistical data are obtained from Table S9–S10. Only significant correlated chemical classes are shown here. A full version of these correlations is included in Supplementary Information Figure S9.

(DLCA) (Norgren and Edlund, 2014). Such hydrophobic aggregates are repelled by the hydrophilic surface of minerals or OM coatings, minimizing their surface contact and associated surface energy (Tanford, 1980). The formation of hydrophobic aggregates is supported by computational molecular dynamics (MD) simulations (Andersen and Laskin, n.d.), suggesting a strong mechanistic basis for our results. Our empirical evidence reveals that condensed hydrocarbon-, lignin-, and tannin-like compounds do not preferentially accumulate in the hydrophobic zone of Fh in grassland soil (Fig. 6).

Amino sugars have been extensively studied as a signature of microbial necromass (Amelung et al., 2008; Liang et al., 2011; Glaser et al., 2004). For instance, chitin, a polymer of amino sugars with units of *N*-acetyl-D-glucosamine, is the residue of mycelia from fungi and actinobacteria; similarly, muramic acid is an amino sugar that is a dominant constituent of bacterial cell walls. Previous studies reported that these signature amino sugars are the foundation for microbial necromass comprising the vast majority of stable MAOM (Kallenbach et al., 2016; Pronk et al., 2015). Our results show a negative correlation between amino sugar-like compounds and Fh content ($p < 0.05$, $n = 24$, Fig. 6 and Table S9), suggesting that amino sugars do not preferentially accumulate to the hydrophobic zone of organo-mineral complexes. This could be caused by the limited sorption sites on mineral surfaces or on OM in the contact zone, as a sorption experiment demonstrated that proteins preferentially bind to mineral surfaces while polysaccharides

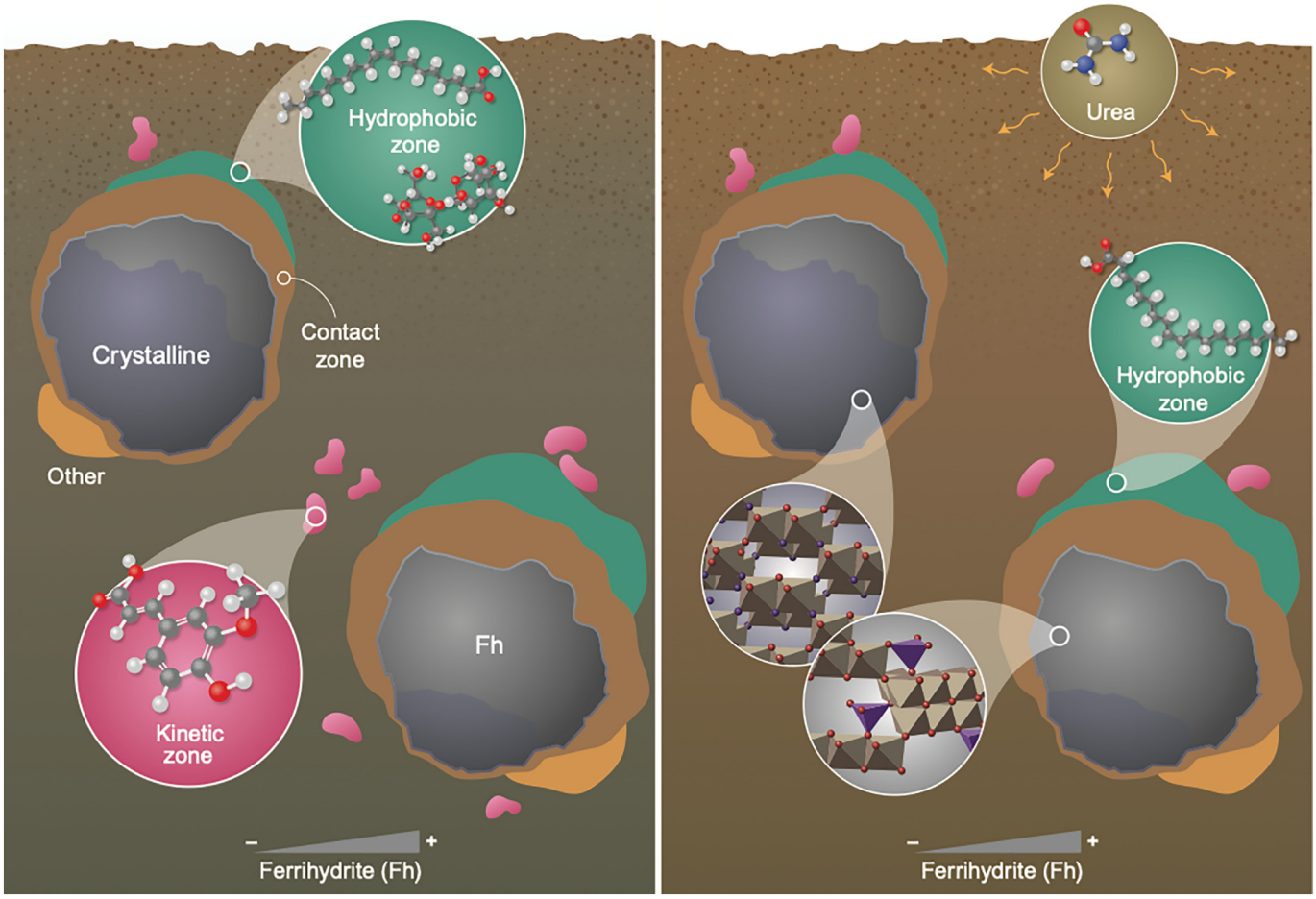

Fig. 7. Conceptual model of how mineral-organic matter interactions are influenced by Fh abundance and N addition. (i) The left panel shows soils with low (upper left) and high (lower right) ferrihydrite (Fh) content under unfertilized conditions. The hydrophobic zone is dominated by protein- and lipid-like molecules, shown in green. The size of the area corresponds to the relative abundance of each component. The kinetic zone is enriched in lignin-like molecules presented in red, with the number of the component corresponding to the relative abundance. (ii) The right panel shows soils under N-fertilization. In the hydrophobic zone, only lipid-like molecules increase with increased Fh content, similar to unfertilized soils. However, in contrast to unfertilized soils, protein-like molecules in hydrophobic zone and lignin-like molecules in the kinetic zone are unrelated to Fh content.

remain in solution (Feng et al., 2005). Therefore, the decomposition of free amino sugars may occur rapidly prior to contact with OM in hydrophobic zone or mineral surface (Pronk et al., 2015; Roberts et al., 2007).

Our results demonstrate that soil minerals play a key role in protecting classes of organic molecules from microbial degradation in predictable ways, which is supported by previous studies. Torn et al. (1997) demonstrated that the abundance of non-crystalline minerals, including Fh, accounted for greater OM content in soil, compared to highly crystalline minerals. Ferrihydrite is enriched in OH groups on the surface layer and has high surface area, which result in a higher sorption affinity to OM, compared to hematite or goethite (Kaiser and Guggenberger, 2000). Moreover, the sorption of SOM by Fe oxides has been proposed to stabilize OM from microbial decomposition and thus play a critical role in C sequestration (Wagai and Mayer, 2007; Jones and Edwards, 1998; Kögel-Knabner et al., 2008). Across a volcanic soil chronosequence, $\Delta^{14}C$ of OM was negatively correlated with abundance of non-crystalline minerals (i.e., greater non-crystalline minerals were associated with older OM) (Torn et al., 1997), illustrating the importance of non-crystalline minerals for long term C stabilization. As discussed above, Fh-bound OM potentially has lower biological availability and long residence times in soil compared to highly crystalline Fe oxide-bound OM. Our study demonstrates that the amount of Fh strongly influences organic C stabilization. More importantly, our results at the landscape scale reveal the chemical nature of the dynamic pool of Fe oxide-associated OM, which is largely composed of lipid- and protein-like molecules.

3.4. Biochemical accumulation of OM in the kinetic zone varies with amount of Fh

OM in the kinetic zone represents the fraction of OM unbound and/or loosely bound to minerals and easily accessed by microbes or subject to transport processes. Across our continental-scale gradient, the chemical composition of kinetic OM predominantly consisted of lignin-like compounds and their abundance was a function of Fh content. The relative contribution of lignin-like compounds in the kinetic zone ranged from 18% to 52% in soils from unfertilized plots across the six sites (Fig. S7). In addition, the relative contribution of lignin-like compounds in the kinetic zone was positively correlated with the amount of Fh ($p < 0.01$, $n = 24$), while carbohydrate- and condensed hydrocarbon-like compounds showed significant negative correlations with the amount of Fh ($p < 0.05$, n = 24) (Figs. S9–S10 and Table S10). Lignin has been considered resistant (energetically unfavorable) to microbial decomposition, because only a limited group of lignolytic fungi (producing laccase and peroxidase enzymes) and bacteria (e.g., Actinomycetes) are capable of completely mineralizing lignin to CO2 (Spiker et al., 1992; Kögel-Knabner, 2002; Viswanath et al., 2014; Datta et al., 2017). In addition to unfavorable energetics of oxidative

degradation (LaRowe and Van Cappellen, 2011) and its biochemically stable nature (Waksman, 1936; Berg and McClaugherty, 2014), the interactions of lignin with minerals and the solubility of lignin-like compounds are important determinants of OM dynamics in grasslands. For instance, we observed a negative correlation of lignin-like compounds in the hydrophobic zone with Fh content (Fig. 5), while the opposite correlation was observed from the kinetic zone, indicating that the mobilization of lignin-like molecules is strongly regulated by the abundance of Fh (Fig. 7). Our results suggest that Fh geochemically preserved protein- and lipid-like compounds in the hydrophobic zone of MAOM rather than lignin-like compounds because of different sorption affinities; however, lignin-like compounds were biochemically accumulated in the kinetic zone because their chemical nature (e.g. high aromaticity and double bond equivalent, large molecule size, and hydrophobicity) makes them unfavorable substrates for microbial assimilation. Therefore, biochemical and geochemical stabilization of OM likely both contribute to the persistence of SOM in grassland soils.

3.5. N enrichment shifts C chemistry and reduces Fe mineral-OM interactions

The predictable interactions of C chemical classes with Fe mineral phases was disrupted by nearly a decade of N fertilization. Addition of 10 g N m^{-2} yr^{-1} (as urea) resulted in unique moieties of C compared to native grassland soils without N fertilization. Specifically, protein-like molecules in the hydrophobic zone of MAOM were positively correlated with the concentration of Fh in unfertilized soils across the six sites, but no correlation was observed in N-fertilized soils (Fig. S11, Table S11). The positive correlation between lignin-like molecules in the kinetic zone and Fh content also was disrupted by the addition of N (Fig. S11, Table S12). On the other hand, N addition did not affect both the positive correlation of lipid-like molecules and the negative correlation of lignin-like molecules in the hydrophobic zone with the content of Fh (Fig. 7, Fig. S11, Table S9 and S11). These results suggest that N addition potentially may alter the chemical structure of Fe minerals or affect the chemical structure of protein-like molecules, resulting in the alteration of mineral-protein interactions. Mössbauer spectra of two N-fertilized samples, representing high and low Fe contents (BG and SV), displayed the same general set of Fe-minerals as unfertilized samples, with strong Pearson correlation coefficients ($r^2 = 0.974$ for BG, $n = 512$; and $r^2 = 0.977$ for SV, $n = 512$) in both soils (Fig. S1), suggesting N addition did not directly cause the transformation of the chemical structure of Fe minerals.

Rather, evidence suggests that N addition changed the sorption of protein to Fh surfaces or OM in the contact zone by altering pH (p-value = 0.02, $n = 48$; Table S13) and thereby changing the surface charge of Fh or other organic functional groups in the contact zone and the extent of protein ionization (Yu et al., 2013). N fertilizer was added as urea, which can be hydrolyzed into ammonium (NH_4^+). The increased NH_4^+ concentration likely stimulated nitrification, releasing hydrogen (H^+) and nitrate (NO_3^-). Decreased pH due to increased proton availability and cation leaching by NO_3^- can invoke several processes that may simultaneously disperse the sorption of proteins on Fh surfaces or OM in the contact zone. First, soils with low pH result in more positive charges on both protein and Fh surfaces or OM in the contact zone (Yu et al., 2013), causing the loss of proteins because of disturbed electrostatic interactions. Second, soil acidification causes the dissolution or release of base cations (Ca^{2+} or Mg^{2+}) by disrupting cation bridging of OM on mineral surfaces (Yu et al., 2017; Ye et al., 2018; Gu et al., 1994). This can result in the release of proteins from Fh surfaces or OM in the contact zone. In contrast, NH_4^+ resulting from addition of urea can be assimilated by plants and microbes that synthesize more proteins that are available for sorption. In addition, decreased pH increases the prevalence of ligand exchange on mineral surfaces by releasing H^+, resulting in more associations of OM, e.g., proteins (Kögel-Knabner et al., 2008; Kleber et al., 2005; Lützow et al., 2006). Therefore, both negative and positive effects of sorption of protein-like molecules on Fh surfaces or OM in the contact zone likely occurred concurrently when urea was applied across the six sites, reducing correlations with soil mineralogy (Fig. 7).

However, altered pH-induced by N addition did not impact correlations of other OM components, such as lignin-like molecules, with Fh in the hydrophobic zone. The underlying mechanism is likely different than that of protein-like molecules. Lignin molecules are largely composed of hydrophobic OM rich in hydroxyl and carboxyl groups and aromatic C, such as phenol and benzenecarboxylic acid. Not only carboxylic and phenolic groups within lignin molecules sorb to OM or mineral surfaces in the contact zone via electrostatic interactions (Gu et al., 1994; Kaiser, 2003; Huang et al., 2019), hydrophobic fractions from lignin also play a role in the sorption to the contact zone or mineral surfaces via hydrophobic forces (Gu et al., 1994; Kaiser, 2003). Under the condition given in this study, H^+ and other cations (Ca^{2+} or Mg^{2+}) released by decreased pH likely sorb to negatively charged OM on the contact zone surface. A neutral surface of the contact zone of MAOM may preferentially sorb hydrophobic fractions via hydrophobic forces and van der Waal forces, compared to hydrophilic fractions of OM (Wu et al., 2008). Therefore, we found that N addition did not alter the correlation of lignin-like molecule (rich in hydrophobic components) in the hydrophobic zone with the Fh content (Fig. S11), although decreased pH may alter electrostatic interactions of hydrophilic fractions. Moreover, a previous study found that hydrophobic fractions of OM rich in acidic groups and aromatic C more strongly sorbed onto selected Fe minerals than hydrophilic fractions of OM low in acidic groups and aromatic C (Kaiser, 2003).

4. Conclusions

This study, for the first time, provides experimental evidence to systematically validate the conceptual model of zonal structure of mineral-OM complexes proposed a decade ago (Six et al., 2002; Kleber et al., 2007). New C likely accumulates in the hydrophobic zone via hydrophobic interactions and in the kinetic zone due to stable chemical nature. Both of these processes are strongly influenced by the mineral core. Our results show both the biochemical preservation of lignin-like molecules from microbial decomposition and the mineral-associated accumulation of protein- and lipid-like compounds across diverse grassland ecosystems (young vs. well-developed soils). These findings assert that molecule class-specific and mineral phase-dependent understanding of mineral-OM interactions are valuable for managing SOM preservation vs. mineralization, which is foundational to grassland productivity and land-atmosphere C exchange. Moreover, we found that N enrichment altered pH and OM interactions with Fe mineral surfaces or with the contact zone on mineral surfaces, which has not been previously included in mechanistic models that mainly consider pools of C, such as fast-decomposing and mineral-associated pools, at much coarser resolution (Luo et al., 2016; Todd-Brown et al., 2013). The understanding of the effect of N fertilization on mineral-OM interactions also informs the development and deployment of future soil C management practices in grassland and arable ecosystems. In particular, reducing N fertilization may retard the loss of mineral-associated C from soils, thereby likely preventing the increasing concentration of atmospheric C. New mechanistic understanding of SOM persistence can facilitate biogeochemical modeling efforts to predict C cycling under a changing environment.

Credit authorship contribution statement

Qian Zhao: Conceptualization, Methodology, Validation, Formal analysis, Investigation, Writing - original draft, Writing - review & editing, Project administration.**Stephen J. Callister:**Conceptualization, Methodology, Validation, Writing - review & editing, Project administration.**Allison M. Thompson:**Methodology, Software, Formal analysis,

Data curation, Writing - review & editing, Visualization.**Ravi K. Kukkadapu:**Methodology, Formal analysis, Investigation, Resources, Writing - review & editing.**Malak M. Tfaily:**Methodology, Formal analysis, Investigation, Resources, Writing - review & editing.**Lisa M. Bramer:**Methodology, Software, Formal analysis, Data curation.**Nikolla P. Qafoku:**Conceptualization, Validation, Writing - review & editing. **Sheryl L. Bell:**Investigation, Resources, Project administration, Writing - review & editing.**Sarah E. Hobbie:**Resources, Writing - review & editing.**Eric W. Seabloom:**Resources, Writing - review & editing.**Elizabeth T. Borer:**Resources, Writing - review & editing.**Kirsten S. Hofmockel:**Conceptualization, Methodology, Validation, Writing - original draft, Writing - review & editing, Project administration, Supervision, Funding acquisition.

Declaration of competing interest

The authors declare that they have no known competing financial interests or personal relationships that could have appeared to influence the work reported in this paper.

Acknowledgment

This work was funded by National Science Foundation (NSF) award to K. S. Hofmockel (NSF-DEB-1556418) and FY16 Laboratory Directed Research and Development program at Pacific Northwest National Laboratory a multiprogram national laboratory operated by Battelle for the U.S. Department of Energy (contract DE-AC05-76RL01830). We thank collaborators from the Nutrient Network (http://nutnet.org) providing us soil property data. We also thank lead investigators, Dana M. Blumenthal (USDA-Agricultural Research Service), Cynthia S. Brown (Colorado State University), Scott L. Collins (University of New Mexico), Julia A. Klein (Colorado State University), Johannes M. H. Knops (University of Nebraska) at each site for operations and maintenance. Coordination and data management of Nutrient Network project have been supported by E. T. Borer, S. E. Hobbie, and E. W. Seabloom from the National Science Foundation Research Coordination Network (NSF-DEB-1042132) and Long-Term Ecological Research (NSF-DEB-1234162 to Cedar Creek LTER) programs, and the UMN Institute on the Environment (DG-0001-13). The research was performed at EMSL, a DOE Office of Science User Facility sponsored by the Office of Biological and Environmental Research.

Appendix A. Supplementary data

Mössbauer spectroscopy modeling and assignments; Microbial community sequencing method and results; Characteristics of 6 unfertilized study sites; Biogeochemical classes of compounds, elemental composition of compounds, and relative contributions (%) of C chemical classes in six soils; Proportions and amounts of Fe mineral phases based upon Mössbauer spectroscopy; Modeled Mössbauer spectra and parameters; XRD spectra; Correlations of C chemical classes with the amount of ferrihydrite; Beta diversity of bacterial and fungal community compositions; The numbers of N-containing compounds and the correlation between the number of N-containing compounds and the amount of ferrihydrite; The abundance of nitrification-relevant phyla; Mean pH of N-fertilized and unfertilized samples. Supplementary data to this article can be found online at https://doi.org/10.1016/j.scitotenv.2020.137839.

References

Abramoff, R., Xu, X., Hartman, M., O'Brien, S., Feng, W., Davidson, E., Finzi, A., Moorhead, D., Schimel, J., Torn, M., Mayes, M.A., 2018. The Millennial model: in search of measurable pools and transformations for modeling soil carbon in the new century. Biogeochemistry 137 (1–2), 51–71.

Adhikari, D., Zhao, Q., Das, K., Mejia, J., Huang, R., Wang, X., Poulson, S.R., Tang, Y., Roden, E.E., Yang, Y., 2017. Dynamics of ferrihydrite-bound organic carbon during microbial reduction. Geochim. Cosmochim. Acta 212, 221–233.

Amelung, W., Brodowski, S., Sandhage-Hofmann, A., Bol, R., 2008. Combining biomarker with stable isotope analyses for assessing the transformation and turnover of soil organic matter. Adv. Agron. 100, 155–250.

Andersen, A.; Laskin, A., Structure of Soil Organic Matter and its Implications for the Formation of Airborne Soil Organic Particles: Insights from Molecular Dynamics Simulations. (To be submitted for publication).

Andersen, A., Reardon, P.N., Chacon, S.S., Qafoku, N.P., Washton, N.M., Kleber, M., 2016. Protein–mineral interactions: molecular dynamics simulations capture importance of variations in mineral surface composition and structure. Langmuir 32 (24), 6194–6209.

Bach, E.M., Hofmockel, K.S., 2014. Soil aggregate isolation method affects measures of intra-aggregate extracellular enzyme activity. Soil Biol. Biochem. 69, 54–62.

Berg, B., McClaugherty, C., 2014. Plant Litter: Decomposition, Humus Formation, Carbon Sequestration. Springer-Verlag, Berlin, Germany.

Bigham, J.M., Fitzpatrick, R.W., Schulze, D.G., 2002. Iron oxides. In: Dixon, J.B., Schulze, D.G. (Eds.), Soil Mineralogy with Environmental Applications. Soil Science Society of America, Madison, WI USA, pp. 323–366.

Borer, E.T., Harpole, W.S., Adler, P.B., Lind, E.M., Orrock, J.L., Seabloom, E.W., Smith, M.D., 2014. Finding generality in ecology: a model for globally distributed experiments. Methods Ecol. Evol. 5 (1), 65–73.

Cagnasso, M., Boero, V., Franchini, M.A., Chorover, J., 2010. ATR-FTIR studies of phospholipid vesicle interactions with α-FeOOH and α-Fe2O3 surfaces. Colloids Surf. B: Biointerfaces 76 (2), 456–467.

Chen, C., Kukkadapu, R., Sparks, D.L., 2015. Influence of coprecipitated organic matter on Fe2+ (aq)-catalyzed transformation of ferrihydrite: implications for carbon dynamics. Environ. Sci. Technol. 49 (18), 10927–10936.

Christensen, B.T., 1996. Carbon in primary and secondary Organomineral complexes. In: Carter, M.R., Stewart, B.A. (Eds.), Structure and Organic Matter Storage in Agricultural Soils. CRC Press, Inc, Boca, Raton, pp. 97–165.

Churchman, G.J., Lowe, D.J., 2012. Alteration, formation, and occurrence of minerals in soils. In: Huang, P.M., Li, Y., Sumner, M.E. (Eds.), Handbook of Soil Sciences-Properties and Processes. CRC Press, Boca Raton, pp. 20–10–20–72.

Conant, R.T., Ryan, M.G., Ågren, G.I., Birge, H.E., Davidson, E.A., Eliasson, P.E., Evans, S.E., Frey, S.D., Giardina, C.P., Hopkins, F.M., 2011. Temperature and soil organic matter decomposition rates–synthesis of current knowledge and a way forward. Glob. Chang. Biol. 17 (11), 3392–3404.

Cornell, R.M., Schwertmann, U., 2003. The Iron Oxides: Structure, Properties, Reactions, Occurrences and Uses. John Wiley & Sons.

Coward, E.K., Thompson, A.T., Plante, A.F., 2017. Iron-mediated mineralogical control of organic matter accumulation in tropical soils. Geoderma 306, 206–216.

Coward, E.K., Ohno, T., Plante, A.F., 2018. Adsorption and molecular fractionation of dissolved organic matter on iron-bearing mineral matrices of varying crystallinity. Environ. Sci. Technol. 52 (3), 1036–1044.

Datta, R., Kelkar, A., Baraniya, D., Molaei, A., Moulick, A., Meena, R.S., Formanek, P., 2017. Enzymatic degradation of lignin in soil: a review. Sustainability 9 (7), 1163.

Dontsova, K., 2009. Solid phase evolution in the Biosphere 2 hillslope experiment as predicted by modeling of hydrologic and geochemical fluxes. Hydrol. Earth Syst. Sci. 13, 2273–2286.

Feng, X., Simpson, A.J., Simpson, M.J., 2005. Chemical and mineralogical controls on humic acid sorption to clay mineral surfaces. Org. Geochem. 36 (11), 1553–1566.

Fernandes de Oliveira, M., Johnston, C.T., Premachandra, G., Teppen, B.J., Li, H., Laird, D.A., Zhu, D., Boyd, S.A., 2005. Spectroscopic study of carbaryl sorption on smectite from aqueous suspension. Environ. Sci. Technol. 39 (23), 9123–9129.

Folch, J., Lees, M., Sloane Stanley, G., 1957. A simple method for the isolation and purification of total lipids from animal tissues. J. Biol. Chem. 226 (1), 497–509.

Gee, G.W., Bauder, J.W., 1986. Particle-size analysis. Methods of Soil Analysis: Part 1 Physical and Mineralogical Methods. 5, pp. 383–411.

Glaser, B., Turrión, M., Alef, K., 2004. Amino sugars and muramic acid—biomarkers for soil microbial community structure analysis. Soil Biol. Biochem. 36 (3), 399–407.

Gu, B., Schmitt, J., Chen, Z., Liang, L., McCarthy, J.F., 1994. Adsorption and desorption of natural organic matter on iron oxide: mechanisms and models. Environ. Sci. Technol. 28 (1), 38–46.

Hatton, P., Kleber, M., Zeller, B., Moni, C., Plante, A.F., Townsend, K., Gelhaye, L., Lajtha, K., Derrien, D., 2012. Transfer of litter-derived N to soil mineral–organic associations: evidence from decadal 15N tracer experiments. Org. Geochem. 42 (12), 1489–1501.

Havlin, J.L., Beaton, J.D., Tisdale, S.L., Nelson, W.L., 2005. Soil Fertility and Fertilizers: An Introduction to Nutrient Management. 7th ed. 515. Prentice Hall, Upper Saddle River, NJ.

Heckman, K., Lawrence, C.R., Harden, J.W., 2018. A sequential selective dissolution method to quantify storage and stability of organic carbon associated with Al and Fe hydroxide phases. Geoderma 312, 24–35.

Hlady, V., Buijs, J., 1996. Protein adsorption on solid surfaces. Curr. Opin. Biotechnol. 7 (1), 72.

Hofmockel, K.S., Schlesinger, W.H., Jackson, R.B., 2007. Effects of elevated atmospheric carbon dioxide on amino acid and NH4+-N cycling in a temperate pine ecosystem. Glob. Chang. Biol. 13 (9), 1950–1959.

Huang, X., Tang, H., Kang, W., Yu, G., Ran, W., Hong, J., Shen, Q., 2018. Redox interface-associated organo-mineral interactions: a mechanism for C sequestration under a rice-wheat cropping system. Soil Biol. Biochem. 120, 12–23.

Huang, X., Chen, Y., Walter, E., Zong, M., Wang, Y., Zhang, X., Qafoku, O., Wang, Z., Rosso, K.M., 2019. Facet-specific photocatalytic degradation of organics by heterogeneous fenton chemistry on hematite nanoparticles. Environ. Sci. Technol. 53 (17), 10197–10207.

Johnston, C.T., Premachandra, G.S., Szabo, T., Lok, J., Schoonheydt, R.A., 2011. Interaction of biological molecules with clay minerals: a combined spectroscopic and sorption study of lysozyme on saponite. Langmuir 28 (1), 611–619.
Jones, D.L., Edwards, A.C., 1998. Influence of sorption on the biological utilization of two simple carbon substrates. Soil Biol. Biochem. 30 (14), 1895–1902.
Jones, E., Singh, B., 2014. Organo-mineral interactions in contrasting soils under natural vegetation. Front. Environ. Sci. 2, 2.
Kaiser, K., 2003. Sorption of natural organic matter fractions to goethite (α-FeOOH): effect of chemical composition as revealed by liquid-state 13C NMR and wet-chemical analysis. Org. Geochem. 34 (11), 1569–1579.
Kaiser, K., Guggenberger, G., 2000. The role of DOM sorption to mineral surfaces in the preservation of organic matter in soils. Org. Geochem. 31 (7–8), 711–725.
Kaiser, K., Guggenberger, G., 2003. Mineral surfaces and soil organic matter. Eur. J. Soil Sci. 54 (2), 219–236.
Kaiser, K., Guggenberger, G., Haumaier, L., Zech, W., 1997. Dissolved organic matter sorption on sub soils and minerals studied by 13C-NMR and DRIFT spectroscopy. Eur. J. Soil Sci. 48 (2), 301–310.
Kallenbach, C.M., Frey, S.D., Grandy, A.S., 2016. Direct evidence for microbial-derived soil organic matter formation and its ecophysiological controls. Nat. Commun. 7, 13630.
Kim, S., Kramer, R.W., Hatcher, P.G., 2003. Graphical method for analysis of ultrahigh-resolution broadband mass spectra of natural organic matter, the van Krevelen diagram. Anal. Chem. 75 (20), 5336–5344.
Kleber, M., Mikutta, R., Torn, M.S., Jahn, R., 2005. Poorly crystalline mineral phases protect organic matter in acid subsoil horizons. Eur. J. Soil Sci. 56 (6), 717–725.
Kleber, M., Sollins, P., Sutton, R., 2007. A conceptual model of organo-mineral interactions in soils: self-assembly of organic molecular fragments into zonal structures on mineral surfaces. Biogeochemistry 85 (1), 9–24.
Kleber, M., Eusterhues, K., Keiluweit, M., Mikutta, C., Mikutta, R., Nico, P.S., 2015. Mineral–organic associations: formation, properties, and relevance in soil environments. In: Sparks, D.L. (Ed.), Advances in Agronomy. 130. Elsevier Academic Press Inc, San Diego, CA, pp. 1–140.
Koch, B.P., Dittmar, T., 2006. From mass to structure: an aromaticity index for high-resolution mass data of natural organic matter. Rapid Commun. Mass Spectrom. 20 (5), 926–932.
Koch, B.P., Dittmar, T., 2016. From mass to structure: an aromaticity index for high-resolution mass data of natural organic matter. Rapid Commun. Mass Spectrom. 30 (5), 250.
Kögel-Knabner, I., 2002. The macromolecular organic composition of plant and microbial residues as inputs to soil organic matter. Soil Biol. Biochem. 34 (2), 139–162.
Kögel-Knabner, I., Guggenberger, G., Kleber, M., Kandeler, E., Kalbitz, K., Scheu, S., Eusterhues, K., Leinweber, P., 2008. Organo-mineral associations in temperate soils: integrating biology, mineralogy, and organic matter chemistry. J. Plant Nutr. Soil Sci. 171 (1), 61–82.
Kramer, M.G., Chadwick, O.A., 2018. Climate-driven thresholds in reactive mineral retention of soil carbon at the global scale. Nat. Clim. Chang. 8 (12), 1104–1108.
Kramer, M.G., Sanderman, J., Chadwick, O.A., Chorover, J., Vitousek, P.M., 2012. Long-term carbon storage through retention of dissolved aromatic acids by reactive particles in soil. Glob. Chang. Biol. 18 (8), 2594–2605.
Krull, E., Baldock, J., Skjemstad, J., 2001. Soil texture effects on decomposition and soil carbon storage. Net Ecosystem Exchange CRC Workshop Proceedings. 2001. Citeseer, pp. 103–110.
Kukkadapu, R.K., Zachara, J.M., Fredrickson, J.K., Kennedy, D.W., 2004. Biotransformation of two-line silica-ferrihydrite by a dissimilatory Fe (III)-reducing bacterium: formation of carbonate green rust in the presence of phosphate. Geochim. Cosmochim. Acta 68 (13), 2799–2814.
Lalonde, K., Mucci, A., Ouellet, A., Gélinas, Y., 2012. Preservation of organic matter in sediments promoted by iron. Nature 483 (7388), 198.
LaRowe, D.E., Van Cappellen, P., 2011. Degradation of natural organic matter: a thermodynamic analysis. Geochim. Cosmochim. Acta 75 (8), 2030–2042.
Leff, J.W., Jones, S.E., Prober, S.M., Barberán, A., Borer, E.T., Firn, J.L., Harpole, W.S., Hobbie, S.E., Hofmockel, K.S., Knops, J.M., 2015. Consistent responses of soil microbial communities to elevated nutrient inputs in grasslands across the globe. Proc. Natl. Acad. Sci. 112 (35), 10967–10972.
Liang, C., Cheng, G., Wixon, D.L., Balser, T.C., 2011. An Absorbing Markov Chain approach to understanding the microbial role in soil carbon stabilization. Biogeochemistry 106 (3), 303–309.
Liu, D., Dong, H., Agrawal, A., Singh, R., Zhang, J., Wang, H., 2016a. Inhibitory effect of clay mineral on methanogenesis by Methanosarcina mazei and Methanothermobacter thermautotrophicus. Appl. Clay Sci. 126, 25–32.
Liu, J., Wang, Z., Sheng, A., Liu, F., Qin, F., Wang, Z.L., 2016b. In situ observation of hematite nanoparticle aggregates using liquid cell transmission electron microscopy. Environ. Sci. Technol. 50 (11), 5606–5613.
Lopes, A., Guilherme, L., 2016. A career perspective on soil management in the Cerrado Region of Brazil. Adv. Agron. 137, 1–72.
Luo, Y., Ahlström, A., Allison, S.D., Batjes, N.H., Brovkin, V., Carvalhais, N., Chappell, A., Ciais, P., Davidson, E.A., Finzi, A., 2016. Toward more realistic projections of soil carbon dynamics by Earth system models. Glob. Biogeochem. Cycles 30 (1), 40–56.
Lützow, M.v., Kögel-Knabner, I., Ekschmitt, K., Matzner, E., Guggenberger, G., Marschner, B., Flessa, H., 2006. Stabilization of organic matter in temperate soils: mechanisms and their relevance under different soil conditions – a review. Eur. J. Soil Sci. 57 (4), 426–445.
Lv, J., Zhang, S., Wang, S., Luo, L., Cao, D., Christie, P., 2016. Molecular-scale investigation with ESI-FT-ICR-MS on fractionation of dissolved organic matter induced by adsorption on iron oxyhydroxides. Environ. Sci. Technol. 50 (5), 2328–2336.
McMahon, S., Anderson, R.P., Saupe, E.E., Briggs, D.E., 2016. Experimental evidence that clay inhibits bacterial decomposers: implications for preservation of organic fossils. Geology 44 (10), 867–870.
Mikutta, R., Kaiser, K., 2011. Organic matter bound to mineral surfaces: resistance to chemical and biological oxidation. Soil Biol. Biochem. 43 (8), 1738–1741.
Mikutta, R., Mikutta, C., Kalbitz, K., Scheel, T., Kaiser, K., Jahn, R., 2007. Biodegradation of forest floor organic matter bound to minerals via different binding mechanisms. Geochim. Cosmochim. Acta 71 (10), 2569–2590.
Morrison, K.D., Misra, R., Williams, L.B., 2016. Unearthing the antibacterial mechanism of medicinal clay: a geochemical approach to combating antibiotic resistance. Sci. Rep. 6, 19043.
Norgren, M., Edlund, H., 2014. Lignin: recent advances and emerging applications. Curr. Opin. Colloid Interface Sci. 19 (5), 409–416.
Oksanen, J., Blanchet, F.G., Kindt, R., Legendre, P., Minchin, P.R., O'hara, R., Simpson, G.L., Solymos, P., Stevens, M.H.H., Wagner, H., 2013. Package 'vegan'. Community Ecology Package, Version. 2, (9).
Parfitt, R., Clayden, B., 1991. Andisols—the development of a new order in soil taxonomy. Geoderma 49 (3–4), 181–198.
Peretyazhko, T.S., Zachara, J.M., Kukkadapu, R.K., Heald, S.M., Kutnyakov, I.V., Resch, C.T., Arey, B.W., Wang, C.M., Kovarik, L., Phillips, J.L., 2012. Pertechnetate (TcO^{4-}) reduction by reactive ferrous iron forms in naturally anoxic, redox transition zone sediments from the Hanford Site, USA. Geochim. Cosmochim. Acta 92, 48–66.
Pronk, G.J., Heister, K., Kögel-Knabner, I., 2015. Amino sugars reflect microbial residues as affected by clay mineral composition of artificial soils. Org. Geochem. 83, 109–113.
Quiquampoix, H., Staunton, S., Baron, M.H., Ratcliffe, R.G., 1993. Interpretation of the pH dependence of protein adsorption on clay mineral surfaces and its relevance to the understanding of extracellular enzyme activity in soil. Colloids Surf. A Physicochem. Eng. Asp. 75, 85–93.
Rancourt, D.G., Ping, J.Y., 1991. Voigt-based methods for arbitrary-shape static hyperfine parameter distributions in Mössbauer spectroscopy. Nucl. Instrum. Methods Phys. Res., Sect. B 58 (1), 85–97.
Rasmussen, C., Heckman, K., Wieder, W.R., Keiluweit, M., Lawrence, C.R., Berhe, A.A., Blankinship, J.C., Crow, S.E., Druhan, J.L., Pries, C.E.H., 2018. Beyond clay: towards an improved set of variables for predicting soil organic matter content. Biogeochemistry 137 (3), 297–306.
Roberts, P., Bol, R., Jones, D.L., 2007. Free amino sugar reactions in soil in relation to soil carbon and nitrogen cycling. Soil Biol. Biochem. 39 (12), 3081–3092.
Rumpel, C., Rodríguez-Rodríguez, A., González-Pérez, J.A., Arbelo, C., Chabbi, A., Nunan, N., González-Vila, F.J., 2012. Contrasting composition of free and mineral-bound organic matter in top-and subsoil horizons of Andosols. Biol. Fertil. Soils 48 (4), 401–411.
Saggar, S., Parshotam, A., Sparling, G., Feltham, C., Hart, P., 1996. 14C-labelled ryegrass turnover and residence times in soils varying in clay content and mineralogy. Soil Biol. Biochem. 28 (12), 1677–1686.
Schmidt, M.W.I., Torn, M.S., Abiven, S., Dittmar, T., Guggenberger, G., Janssens, I.A., Kleber, M., Kögel-Knabner, I., Lehmann, J., Manning, D.A.C., Nannipieri, P., Rasse, D.P., Weiner, S., Trumbore, S.E., 2011. Persistence of soil organic matter as an ecosystem property. Nature 478, 49–56.
Schneider, M.P.W., Scheel, T., Mikutta, R., Van Hees, P., Kaiser, K., Kalbitz, K., 2010. Sorptive stabilization of organic matter by amorphous Al hydroxide. Geochim. Cosmochim. Acta 74 (5), 1606–1619.
Six, J., Elliott, E., Paustian, K., 2000. Soil macroaggregate turnover and microaggregate formation: a mechanism for C sequestration under no-tillage agriculture. Soil Biol. Biochem. 32 (14), 2099–2103.
Six, J., Conant, R.T., Paul, E.A., Paustian, K., 2002. Stabilization mechanisms of soil organic matter: implications for C-saturation of soils. Plant Soil 241 (2), 155–176.
Sparks, D.L., 2003. Environmental Soil Chemistry. 2nd ed. Academic Press, San Diego, CA.
Spiker, J.K., Crawford, D.L., Thiel, E.C., 1992. Oxidation of phenolic and non-phenolic substrates by the lignin peroxidase of *Streptomyces viridosporus* T7A. Appl. Microbiol. Biotechnol. 37 (4), 518–523.
Sposito, G., Skipper, N.T., Sutton, R., Park, S.-h., Soper, A.K., Greathouse, J.A., 1999. Surface geochemistry of the clay minerals. Proc. Natl. Acad. Sci. 96 (7), 3358–3364.
Stenson, A.C., Marshall, A.G., Cooper, W.T., 2003. Exact masses and chemical formulas of individual Suwannee River fulvic acids from ultrahigh resolution electrospray ionization Fourier transform ion cyclotron resonance mass spectra. Anal. Chem. 75 (6), 1275–1284.
Stevenson, F.J., 1995. Humus Chemistry: Genesis, Composition, Reactions. 2nd ed. 72. American Chemical Society, p. A93.
Tanford, C., 1980. The Hydrophobic Effect: Formation of Micelles and Biological Membranes. 2nd ed. Wiley, New York, p. 233.
Tfaily, M.M., Chu, R.K., Tolić, N., Roscioli, K.M., Anderton, C.R., Paša-Tolić, L., Robinson, E.W., Hess, N.J., 2015. Advanced solvent based methods for molecular characterization of soil organic matter by high-resolution mass spectrometry. Anal. Chem. 87 (10), 5206–5215.
Tfaily, M.M., Chu, R.K., Toyoda, J., Tolić, N., Robinson, E.W., Paša-Tolić, L., Hess, N.J., 2017. Sequential extraction protocol for organic matter from soils and sediments using high resolution mass spectrometry. Anal. Chim. Acta 972, 54–61.
Thompson, A., Chadwick, O.A., Rancourt, D.G., Chorover, J., 2006. Iron-oxide crystallinity increases during soil redox oscillations. Geochim. Cosmochim. Acta 70 (7), 1710–1727.
Todd-Brown, K.E., Randerson, J.T., Post, W.M., Hoffman, F.M., Tarnocai, C., Schuur, E.A., Allison, S.D., 2013. Causes of variation in soil carbon simulations from CMIP5 Earth system models and comparison with observations. Biogeosciences 10 (3), 1717–1736.
Torn, M.S., Trumbore, S.E., Chadwick, O.A., Vitousek, P.M., Hendricks, D.M., 1997. Mineral control of soil organic carbon storage and turnover. Nature 389 (6647), 170.

Viswanath, B., Rajesh, B., Janardhan, A., Kumar, A.P., Narasimha, G., 2014. Fungal laccases and their applications in bioremediation. Enzym. Res. 2014.
von Lützow, M., Kögel-Knabner, I., Ludwig, B., Matzner, E., Flessa, H., Ekschmitt, K., Guggenberger, G., Marschner, B., Kalbitz, K., 2008. Stabilization mechanisms of organic matter in four temperate soils: development and application of a conceptual model. J. Plant Nutr. Soil Sci. 171 (1), 111–124.
Wagai, R., Mayer, L.M., 2007. Sorptive stabilization of organic matter in soils by hydrous iron oxides. Geochim. Cosmochim. Acta 71 (1), 25–35.
Waksman, S.A., 1936. Humus Origin, Chemical Composition, and Importance in Nature. Waverly Press, BALTIMORE, MD.
Witt, C., Gaunt, J.L., Galicia, C.C., Ottow, J.C., Neue, H.-U., 2000. A rapid chloroform-fumigation extraction method for measuring soil microbial biomass carbon and nitrogen in flooded rice soils. Biol. Fertil. Soils 30 (5–6), 510–519.
Wong, D., Suflita, J., McKinley, J., Krumholz, L., 2004. Impact of clay minerals on sulfate-reducing activity in aquifers. Microb. Ecol. 47 (1), 80–86.
Wu, H., Lin, Y., Wu, J., Zeng, L., Zeng, D., Du, J., 2008. Surface adsorption of iron oxide minerals for phenol and dissolved organic matter. Earth Sci. Front. 15 (6), 133–141.
Wu, H., Chen, W., Rong, X., Cai, P., Dai, K., Huang, Q., 2014. Soil colloids and minerals modulate metabolic activity of Pseudomonas putida measured using microcalorimetry. Geomicrobiol J. 31 (7), 590–596.
Xu, X., Shi, Z., Li, D., Rey, A., Ruan, H., Craine, J.M., Liang, J., Zhou, J., Luo, Y., 2016. Soil properties control decomposition of soil organic carbon: results from data-assimilation analysis. Geoderma 262, 235–242.
Ye, C., Chen, D., Hall, S.J., Pan, S., Yan, X., Bai, T., Guo, H., Zhang, Y., Bai, Y., Hu, S., 2018. Reconciling multiple impacts of nitrogen enrichment on soil carbon: plant, microbial and geochemical controls. Ecol. Lett. 21 (8), 1162–1173.
Yu, W.H., Li, N., Tong, D.S., Zhou, C.H., Lin, C.X.C., Xu, C.Y., 2013. Adsorption of proteins and nucleic acids on clay minerals and their interactions: a review. Appl. Clay Sci. 80, 443–452.
Yu, G., Xiao, J., Hu, S., Polizzotto, M.L., Zhao, F., McGrath, S.P., Li, H., Ran, W., Shen, Q., 2017. Mineral availability as a key regulator of soil carbon storage. Environ. Sci. Technol. 51 (9), 4960–4969.
Zhao, Q., Poulson, S.R., Obrist, D., Sumaila, S., Dynes, J.J., McBeth, J.M., Yang, Y., 2016. Iron-bound organic carbon in forest soils: quantification and characterization. Biogeosciences 13 (16), 4777–4788.
Zimmerman, A.R., Chorover, J., Goyne, K.W., Brantley, S.L., 2004. Protection of mesopore-adsorbed organic matter from enzymatic degradation. Environ. Sci. Technol. 38 (17), 4542–4548.